is related to the presence of the imidazole function. This proposal can be used not only to explain the aforementioned results of Casella and the findings in this paper, but also the broadened signals in the ^{1}H NMR spectra (298 K) of [Cu(I){imidazole-4-CH_2SR}$_2$]$^+$ complex cations for which intermediate exchange processes can be excluded.[48] As a possible explanation we suggest that in copper(I) imidazole complexes there is an equilibrium involving an intramolecular metal-to-ligand electron shift, i.e., between diamagnetic Cu(I)–imidazole and paramagnetic Cu(II)–imidazole$^{\bullet-}$.[49] Although such an equilibrium can lie far to the side of Cu(I), a small population of the other state can be sufficient to cause extensive line broadening in the NMR spectra. The electron shift equilibrium might facilitate Cu(I)/Cu(II) redox transitions, this perhaps being the reason that nature favors imidazole (over pyridine, pyrazole, or whatever N atom donor) as a coordinating function for copper ions.

Conclusions

Coordination complexes from 1:1 metal salt to ligand reactions of $Ag^IO_3SCF_3$ and the polydentate donor ligand system *N*-[*N*-((5-R-thienyl)methylidene)-L-methionyl]histamine (=(5R)Th-Met-Histam; R = H, Me, Me_3Si) possess intriguing helical polycationic structures, both in the solid state and in solution. The origin of the self-organization relates to the specific structure of the (5R)Th-Met-Histam molecule, which, as a result of steric constraints and the number, nature, and partitioning of its donor and acceptor functions, is preorganized to coordinate to three different Ag(I) cations.

A noteworthy aspect of the complex structure is its complete stereoregularity that is induced by the ligand's single stereogenic carbon center. The corresponding Cu(I) complexes are isostructural to their Ag(I) counterparts. In addition to the oligoligand approach,[3,4] the present self-assembly mechanism provides a second option for the preparation of polycationic coordination complexes.

Acknowledgment. The Netherlands Foundation for Chemical Research (SON) and the Netherlands Organization for Scientific Research (NWO) are thanked for financial support. We gratefully acknowledge the assistance of Prof. Dr. N. M. M. Nibbering and R. Fokkens concerning the ^{252}Cf-PDMS experiment and of Dr. H. P. J. M. Dekkers (University of Leiden) with the CD measurements. Thanks are also due to J.-M. Ernsting for recording the 250-MHz ^{1}H NMR spectra, to A. J. M. Duisenberg for X-ray data collection, to Dr. C. J. Elsevier for helpful discussions, and to Dr. D. M. Grove for his careful reading of the manuscript.

Registry No. ([Ag{(5Me)Th-Met-Histam}]$^+$[OTf]$^-$MeOH), 124781-00-6; [Ag{(5Me)Th-Met-Histam}](OTf), 124780-99-0; [Ag{(5H)Th-Met-Histam}](OTf), 139100-67-7; [Ag{(5Me_3Si)Th-Met-Histam}](OTf), 139100-69-9; [Cu{(5H)Th-Met-Histam}](OTf), 139100-71-3; [Cu{(5Me)Th-Met-Histam}](OTf), 139100-73-5; [Cu{(5Me_3Si)Th-Met-Histam}](OTf), 139100-75-7; ^{109}Ag, 14378-38-2.

Supplementary Material Available: Three ORTEP plots (50% probability) and tables giving refined parameters, bond distances, bond angles, and thermal motion parameters (8 pages); a listing of observed and calculated structure factors (21 pages). Ordering information is given on any current masthead page.

(48) Modder, J. F.; de Klerk-Engels, B.; Ankersmit, H. A.; Vrieze, K.; van Koten, G. *New J. Chem.* **1991**, *15*, 919–926.

(49) (a) The reduction of the imidazole ring upon binding of H$^+$: Grimmett, M. R. *Comprehensive Heterocyclic Chemistry*; Potts, K. T. Ed.; Pergamon Press: New York, 1984; Vol. 5, p 361. (b) The Cu(I)–imidazole MLCT band in: Sorrell, T. N.; Borovik, A. S. *J. Am. Chem. Soc.* **1987**, *109*, 4255–4260.

Contribution from the Departments of Chemistry, University of Western Ontario, London, Ontario, Canada N6A 5B7, and Lakehead University, Thunder Bay, Ontario, Canada P7B 5E1

Protonation of a Metal–Metal Bond Can Lead to Bond Shortening

David J. Elliot,[1a] Jagadese J. Vittal,[1a] Richard J. Puddephatt,*[,1a] David G. Holah,[1b] and Alan N. Hughes[1b]

Received October 16, 1991

The complex [CoRh(CO)$_3$(μ-dppm)$_2$] (**1**) is easily protonated to give [CoRh(μ-H)(CO)$_3$(μ-dppm)$_2$]$^+$ (**2**). The structure of **2**[BF_4] has been determined crystallographically [space group $P\bar{1}$, a = 12.673 (2) Å, b = 19.833 (3) Å, c = 11.992 (3) Å, α = 94.29 (2)°, β = 117.08 (2)°, γ = 107.93 (1)°, Z = 2, R = 0.0519, R_w = 0.0558] and it is shown that the Co–Rh bond is shorter in **2** than in **1**. This is the first example of such a bond shortening on protonation of a metal–metal bond and reasons for the unique behavior are discussed. Complex **2** exhibits fluxionality in solution and it is suggested that this occurs by inversion of the CoRh(μ-H) unit.

Introduction

Protonation of a metal–metal bond has been thought always to lead to an increase in metal–metal bond distance. For example, early work showed that the metal–metal distance in [Cr_2(μ-H)(CO)$_{10}$]$^-$ [3.406 (9) Å] was 0.44 Å longer than in [Cr_2(CO)$_{10}$]$^{2-}$ [2.97 (1) Å].[2] The same effect has been observed in several complexes bridged by bis(diphenylphosphino)methane and related ligands.[3] Thus, the metal–metal bond distance in [RhRe(CO)$_4$(μ-dppm)$_2$] [2.7919 (6) Å] is 0.21 Å shorter than that in [RhRe(μ-H)(CO)$_4$(μ-dppm)$_2$]$^+$ [3.0036 (7) Å].[3] When protonated metal–metal distances are shorter than other metal–metal distances in the same molecule, there are other bridging groups in the MM′(μ-H)(μ-X) unit which cause the effect; that is, the bond-shortening effect of μ-X may outweigh the bond-lengthening effect of μ-H.[4] In these cases, it is presumed that deprotonation would lead to a still shorter metal–metal distance although good structural data for both protonated and deprotonated forms are lacking. The lengthening of a metal–metal bond upon protonation is expected in terms of conversion of a 2c–2e bond to a 3c–2e bond as depicted in eq 1.[4]

(1) (a) University of Western Ontario. (b) Lakehead University.

(2) (a) Handy, L. B.; Ruff, J. K.; Dahl, L. F. *J. Am. Chem. Soc.* **1970**, *92*, 7312. (b) Roziere, J.; Williams, J. M.; Stewart, R. P., Jr.; Petersen, J. L.; Dahl, L. F. *J. Am. Chem. Soc.* **1977**, *99*, 4497.

(3) (a) Antonelli, D. M.; Cowie, M. *Organometallics* **1990**, *9*, 1818. (b) Antonelli, D. M.; Cowie, M. *Inorg. Chem.* 4039. (c) de Leeuw, G.; Field, J. S.; Haines, R. J. *J. Organomet. Chem.* **1989**, *359*, 245. (d) Field, J. S.; Haines, R. J.; Rix, L. A. *J. Chem. Soc., Dalton Trans.* **1990**, 2311.

(4) (a) Churchill, M. R. *Adv. Chem. Ser.* **1978**, *167*, 36. (b) Churchill, M. R.; DeBoer, B. G.; Rotella, F. J. *Inorg. Chem.* **1976**, *15*, 1843. (c) Bau, R.; Don, B.; Greatrex, R.; Haines, R. J.; Love, R. A.; Wilson, R. D. *Inorg. Chem.* **1975**, *14*, 3021.

0020-1669/92/1331-1247$03.00/0

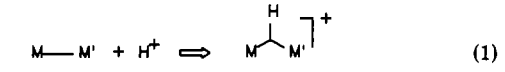

(1)

It is therefore of considerable interest that the protonation of the Co–Rh bond in complex **1**[5] to give **2** (eq 2) occurs with a slight shortening in the Co–Rh bond distance.

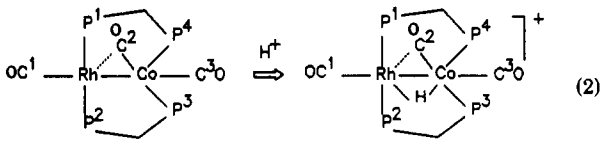

(2)

1 **2**

Structure and Bonding in Complex 2

The structure of **2** is shown in Figure 1, and selected molecular dimensions are given in Table I. A comparison of structural data for **1**[5] and **2** is given in Table II. The major change in geometry which occurs on protonation of **1** is an increase in the P^3–Co–P^4 angle from 108.88 (4) to 131.98 (6)° in **2**, as the coordination number at cobalt increases and the phosphines adopt trans positions in a very highly distorted octahedral stereochemistry (counting both hydride and the metal–metal bond). However, the most intriguing feature is the shortening of the Co–Rh distance from 2.6852 (7) to 2.6480 (8) Å [i.e. by 0.0372 (15) Å] on protonation of **1**. This appears to be the first example of protonation of a metal–metal bond with significant bond shortening. The only other example where such bond shortening may occur is in the closely related complexes $[Rh_2(CO)_3(\mu\text{-dppm})_2]$ (**3**) and $[Rh_2(CO)_2(\mu\text{-H})(\mu\text{-CO})(\mu\text{-dppm})_2]^+$ (**4**) with d(Rh–Rh) = 2.739 (1) and 2.731 (2) Å, respectively, but the difference here is not significant.[6]

Another unusual feature of the structure and IR spectrum of **2** concerns the semibridging carbonyl C(2)O(2). The angle Co–C(2)–O(2) decreases from 166.8 (4)° in **1** to 159.5 (5)° in **2**, indicating that the carbonyl is more strongly bridging in **2**. This conclusion is also supported by the significant decrease in the distance Rh–C(2) and the increase in the distance Co–C(2) in **2** compared to **1** (Table II). However, ν(CO) for this carbonyl (C(2)O(2)) increases from 1815 cm^{-1} in **1** to 1933 cm^{-1} in **2**, whereas the terminal carbonyl stretching frequencies increase only from 1965, 1922 cm^{-1} in **1** to 1981, 1946 cm^{-1} in **2**. This indicates that back-bonding to the semibridging carbonyl is much weaker in **2** than in **1**. Back-bonding to all carbonyls is, of course, expected to be weaker in **2** than in **1** since **2** is a cation and since the formal oxidation state of cobalt is higher than that in **1**. However, it is surprising that the greatest effect by far is on the semibridging carbonyl, since it bridges more symmetrically in **2** than in **1** and such bridging would be expected to lower ν(CO).

The hydride ligand in **2** was located and refined successfully in the structure determination (see Experimental Section). The difference in bond distances d(RhH) – d(CoH) = 1.84 (5) – 1.54 (5) = 0.30 Å, while the difference in covalent bond radii of rhodium and cobalt is only 0.10 Å. This clearly suggests that the hydride is more strongly bonded to cobalt, although it should be noted that metal–hydrogen distances are not accurately determined by X-ray techniques. In agreement, protonation of **1** to give **2** has a much greater effect on the stereochemistry about cobalt than about rhodium (Table II). Complex **1** has been formulated with a polar donor–acceptor metal–metal bond in which the $Co(CO)_2P_2^-$ unit is the donor and the $Rh(CO)P_2^+$ unit is the acceptor. The proton is expected to add to the point of maximum electron density, and so the stronger bonding to cobalt in **2** is easily rationalized.

Why does the Rh–Co bond become shorter on protonation? The metal–metal bond in **1** has been formulated as donor–acceptor bond, with $Co(CO)_2P_2^-$ as donor and $Rh(CO)P_2^+$ as acceptor,[5] and so the possibility that such bonds might behave in a different way compared to less polar metal–metal bonds should be considered. First, the only precedent is the complex $[RhRe(CO)_4(\mu\text{-dppm})_2]$, which is formulated with a Re→Rh donor–acceptor bond and in which the Re–Rh distance *increases* by 0.21 Å on protonation.[3] It is reasonable that protonation of such a bond should lead to bond weakening since protonation of the anionic rhenium $[Re(CO)_3P_2^-]$ center to give a neutral $ReH(CO)_3P_2$ unit would make this a weaker donor and so give a weaker metal–metal bond. Note that the bond could be considered to be formed by donation of two electrons from the Re–H bond of the $ReH(CO)_3P_2$ unit to the $Rh(CO)P_2^+$ acceptor [an agostic interaction], but the net result is still a 3c–2e MM′(μ-H) bond which is longer than the corresponding 2c–2e MM′ bond. Thus, there is no reason to expect, on the basis of either precedent or theory, that a donor–acceptor and a covalent metal–metal bond will behave differently on protonation.

It is significant that, in both protonated complexes **2** and **4**, the carbonyl C(2)O(2) is more symmetrically bridging than in the neutral precursors **1** and **3**, respectively, and this effect appears

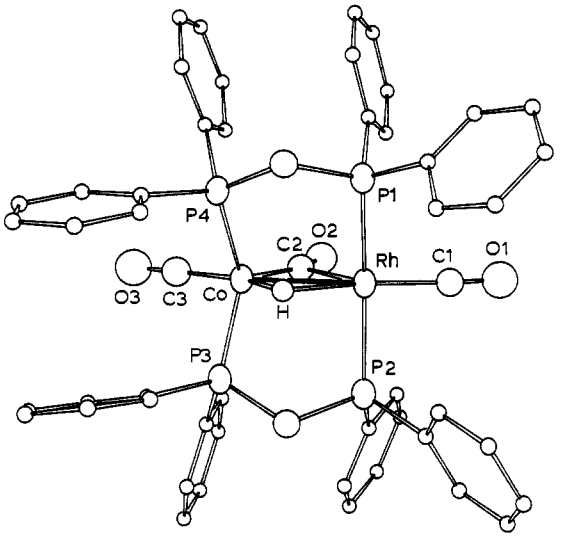

Figure 1. View of the structure of $[CoRh(\mu\text{-H})(\mu\text{-CO})(CO)_2(\mu\text{-dppm})_2]^+$. Carbon atoms of the phenyl rings and the hydride atom are shown as spheres of arbitrary radius while other atoms are represented by 50% probability ellipsoids.

Table I. Selected Bond Distances (Å) and Angles (deg) for **2**

		Distances	
Rh–Co	2.6480 (8)	Rh–P(1)	2.312 (1)
Rh–P(2)	2.318 (1)	Rh–H(1)	1.84 (5)
Rh–C(1)	1.858 (13)	Rh–C(1a)	1.860 (18)
Rh–C(2)	2.279 (6)	Co–P(3)	2.185 (2)
Co–P(4)	2.189 (2)	Co–H(1)	1.54 (5)
Co–C(2)	1.796 (6)	Co–C(3)	1.720 (6)
O(1)–C(1)	1.134 (14)	O(1a)–C(1a)	1.141 (20)
O(2)–C(2)	1.153 (7)	O(3)–C(3)	1.162 (7)
		Angles	
P(1)–Rh–Co	90.68 (4)	P(2)–Rh–Co	90.94 (4)
C(1)–Rh–Co	158.7 (4)	C(1a)–Rh–Co	171.0 (6)
C(2)–Rh–Co	41.9 (1)	P(2)–Rh–P(1)	162.71 (6)
C(1)–Rh–P(1)	94.2 (4)	C(1a)–Rh–P(1)	87.5 (5)
C(2)–Rh–P(1)	96.4 (1)	C(1)–Rh–P(2)	90.5 (4)
C(1a)–Rh–P(2)	93.4 (5)	C(2)–Rh–P(2)	96.3 (1)
C(1a)–Rh–C(1)	13.7 (6)	C(2)–Rh–C(1)	116.8 (4)
C(2)–Rh–C(1a)	129.6 (6)	P(3)–Co–Rh	97.48 (5)
P(4)–Co–Rh	97.51 (5)	C(2)–Co–Rh	58.0 (2)
C(3)–Co–Rh	160.1 (2)	P(4)–Co–P(3)	131.98 (6)
C(2)–Co–P(3)	113.8 (2)	C(3)–Co–P(3)	90.5 (2)
C(2)–Co–P(4)	112.8 (2)	C(3)–Co–P(4)	90.4 (2)
C(3)–Co–C(2)	102.2 (3)	Co–H(1)–Rh	102.9 (25)
O(1)–C(1)–Rh	176.6 (12)	O(1a)–C(1a)–Rh	175.2 (18)
Co–C(2)–Rh	80.1 (2)	O(2)–C(2)–Rh	120.3 (4)
O(2)–C(2)–Co	159.5 (5)	O(3)–C(3)–Co	179.3 (6)

(5) Elliot, D. J.; Ferguson, G.; Holah, D. G.; Hughes, A. N.; Jennings, M. C.; Magnuson, V. R.; Potter, D.; Puddephatt, R. J. *Organometallics* **1990**, *9*, 1336.

(6) (a) Woodcock, C.; Eisenberg, R. *Inorg. Chem.* **1985**, *24*, 1285. (b) Kubiak, C. P.; Woodcock, C.; Eisenberg, R. *Inorg. Chem.* **1982**, *21*, 2119.

Table II. Comparison of Molecular Dimensions in Complexes **1**[4] and **2**

	distances, Å			angles, deg	
	1	**2**		**1**	**2**
Rh–Co	2.6852 (7)	2.6480 (8)	Co–C(2)–O	166.8 (4)	159.5 (5)
Rh–C(2)	2.420 (4)	2.279 (6)	Rh–C(2)–O	114.6 (3)	120.3 (4)
Co–C(2)	1.735 (4)	1.796 (6)	Rh–Co–C(2)	62.06 (13)	58.0 (2)
Rh–C(1)	1.846 (4)	1.858 (13)	Co–Rh–C(2)	39.3 (1)	41.9 (1)
Co–C(3)	1.748 (5)	1.720 (6)	P(3)–Co–P(4)	108.88 (4)	131.98 (6)
Rh–P	2.306 (1)	2.312 (1)	P(1)–Rh–P(2)	167.69 (4)	162.71 (6)
	2.309 (1)	2.318 (1)	C(2)–Co–P	125.05 (13)	113.8 (2)
Co–P	2.173 (1)	2.185 (2)		118.06 (14)	112.8 (2)
	2.183 (1)	2.189 (2)	C(3)–Co–P	99.52 (17)	90.5 (2)
				100.41 (16)	90.4 (2)

to be associated with the anomalous metal–metal distances. Formulation of the neutral complexes with a symmetrically bridging carbonyl requires a metal–metal bond order of 0 (16e configuration at each metal) or 2 (18e configuration at each metal, **5** in eq 3). Protonation of the hypothetical latter form would give a complex with a formal metal–metal bond plus a 3c–2e MHM′ bond (**6** in eq 3; M = Rh or Co) and so a shorter metal–metal bond than that in **1** or **3** can be rationalized. The argument is that, in the protonated form, **6** is a more important canonical form than **8** (eq 4) whereas, in the conjugate base, **7** is more important than **5**. Thus, the more symmetrical bridging of the carbonyl in **2** compared to **1** reflects the increasing contribution of the 18e–18e configuration with its stronger metal–metal bonding. If this interpretation is correct, the shortening of a metal–metal bond on protonation will be expected only if the parent complex has a 16e–18e configuration for the two metal atoms as in **1** (eq 1) and only if a ligand like CO becomes more symmetrically bridging in the protonated form. It is therefore likely to continue to be a rare occurrence.

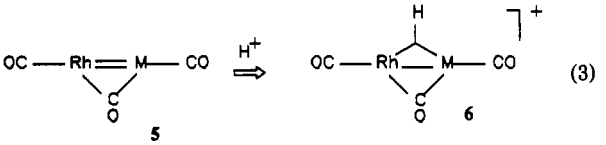

(3)

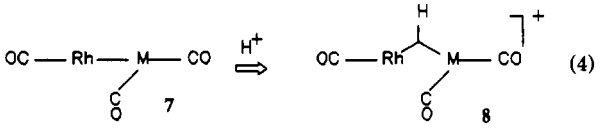

(4)

The halogen- or sulfide-bridged complexes $[Rh_2(\mu\text{-Cl})(\mu\text{-CO})(CO)_2(\mu\text{-dppm})_2]^+$ and $[Ir_2(\mu\text{-S})(\mu\text{-CO})(CO)_2(\mu\text{-dppm})_2]$ should have single metal–metal bonds, and the bond lengths are significantly longer than those in $[Rh_2(\mu\text{-H})(\mu\text{-CO})(CO)_2(\mu\text{-dppm})_2]^+$ and $[Ir_2(\mu\text{-H})(\mu\text{-CO})(CO)_2(\mu\text{-dppm})_2]^+$, respectively.[6-8] Molecular orbital studies at the extended Huckel level predict very similar metal–metal overlap for the halogen-bridged and hydride-bridged complexes, but this does not appear to be consistent with the trend in metal–metal distances.[8]

Fluxionality of 2

The solid-state structure of **2** has three nonequivalent carbonyls and nonequivalent $CH^aH^bP_2$ protons of the μ-dppm ligands. However, the room-temperature ^{13}C NMR spectrum showed only two carbonyl resonances in a 2:1 ratio, and the ^1H NMR spectrum contained a single CH_2P_2 resonance. The spectra were broader but otherwise unchanged at −90 °C. The carbonyl signal with intensity of 2 was broad while that with intensity 1 was sharp and gave a well-defined coupling $^1J(RhC) = 61$ Hz. This defines the fluxional process as exchanging the semibridging carbonyl and terminal CoCO carbonyl without involving the terminal RhCO group. The apparent equivalence of the CH_2P_2 protons indicates that the fluxional process involves an intermediate or transition state with a plane of symmetry containing the $CoRhP_4C_2$ atoms. The simplest mechanism which gives the observed results is one in which the $CoRh(\mu\text{-H})$ unit inverts and the semibridging and terminal carbonyl exchange simultaneously as shown in eq 5. Similar hydride inversion was first detected in the cation $[Pt_2H_2(\mu\text{-H})(\mu\text{-dppm})_2]^+$ and has since been proposed in several other cases.[3,9]

Table III. Summary of X-ray Structure Determination of **2**

compound; fw	$C_{53}H_{45}B_1Co_1F_4O_3P_4Rh$; 1102.49
cryst syst; space group	triclinic; $P\bar{1}$ (No. 2)
cell dimens	
a, Å	12.673 (2)
b, Å	19.833 (3)
c, Å	11.992 (3)
α, deg	94.29 (2)
β, deg	117.08 (2)
γ, deg	107.93 (1)
cell volume, Å^{-3}; Z	2469.8 (3), 2
density, g cm^{-3}: obsd; calcd	1.52 (5); 1.482
radiation; wavelength, Å	Mo $K\alpha_1$; 0.71073
abs coeff, cm^{-1}	7.8
abs max–min	99.78–93.84
final model: R; R_w	0.0519; 0.0558

[a] $R = \sum||F_o| - |F_c||/\sum|F_o|$; $R_w = [\sum w(|F_o| - |F_c|)^2/\sum w|F_o|^2]^{1/2}$; $w = 1/\sigma^2(|F_o|)$.

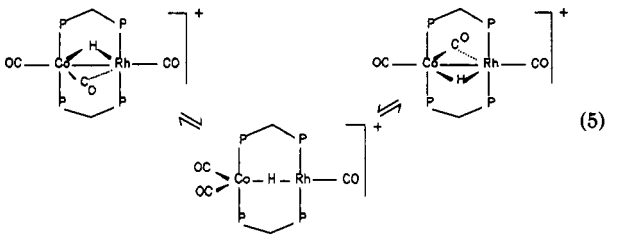

(5)

Experimental Section

The synthesis was carried out in an atmosphere of N_2 using Schlenk techniques. NMR spectra were recorded by using Varian XL200 or XL300 spectrometers.

$[CoRh(\mu\text{-H})(CO)_3(\mu\text{-dppm})_2][BF_4]$. To a solution of $[CoRh(CO)_3(\mu\text{-dppm})_2]$[5] in CH_2Cl_2 (15 mL) was added excess aqueous HBF_4 (1 mL). The reaction mixture was immediately evaporated to dryness under vacuum, and the residue was washed with cold ethanol (1 mL) and recrystallized from CH_2Cl_2/hexane. Yield: 35%. Anal. Calcd for $C_{53}H_{45}BCoF_4O_3P_4Rh$: C, 57.7; H, 4.1 Found: C, 57.4; H, 4.0. NMR in CD_2Cl_2: $\delta(^1H) = -13.3$ [br s, 1 H, $CoRh(\mu\text{-H})$], 3.80 [s, 4 H, CH_2P_2]; $\delta(^{13}C) = 206.9$ [s, 2 C, CoCO], 182.0 [dt, 1 C, $^1J(RhC) = 61$ Hz, $^2J(PC) = 14.5$ Hz, RhCO]; $\delta(^{31}P) = 42.5$ [t, $J_{obs}(PP) = 56.5$ Hz, CoP], 23.1 [dt, $^1J(RhP) = 111$ Hz, $J_{obs}(PP) = 56.5$ Hz, RhP]. IR (Nujol): $\nu(CO) = 1981$ (s), 1946 (sh), 1933 (m) cm^{-1}.

X-ray Structure Determination. A dark red crystal (0.14 × 0.21 × 0.29) was mounted on a glass fiber and transferred to an Enraf-Nonius CAD4 diffractometer for data collection. The crystal density was determined by the neutral buoyancy method using a mixture of carbon tetrachloride and hexane. Unit cell parameters at 23 °C and the orien-

(7) Sutherland, B. R.; Cowie, M. *Can. J. Chem.* **1986**, *64*, 464.
(8) Hoffman, D. M.; Hoffman, R. *Inorg. Chem.* **1981**, *20*, 3543.
(9) Puddephatt, R. J.; Azam, K. A.; Hill, R. H.; Brown, M. P.; Nelson, C. D.; Moulding, R. P.; Seddon, K. R.; Grossel, M. C. *J. Am. Chem. Soc.* **1983**, *105*, 5642.

Table IV. Selected Atomic Positional (×10⁴) and Thermal (×10³) Parameters for **2**

atom	*x*	*y*	*z*	*U*, Å²[a]
Rh	7455.0 (4)	7006.9 (2)	3116.5 (4)	28.2 (2)*
Co	8387.8 (7)	7214.5 (4)	5645.3 (7)	27.5 (3)*
P(1)	7688 (1)	8219 (1)	3270 (1)	30 (1)*
P(2)	7818 (1)	5934 (1)	3004 (1)	31 (1)*
P(3)	9326 (1)	6433 (1)	5937 (1)	28 (1)*
P(4)	9155 (1)	8414 (1)	6153 (1)	28 (1)*
H(1)	8918 (45)	7347 (25)	4717 (44)	21 (13)
C(10)	9179 (5)	8775 (3)	4788 (5)	33 (1)
C(20)	9343 (5)	6091 (3)	4482 (5)	32 (1)
C(1)[b]	6247 (13)	6701 (7)	1359 (12)	36 (3)
O(1)[b]	5469 (10)	6521 (5)	301 (9)	62 (3)
C(1a)[b]	6562 (17)	6856 (10)	1327 (17)	31 (5)
O(1a)[b]	5939 (14)	6731 (8)	229 (13)	58 (4)
C(2)	6693 (6)	6813 (3)	4507 (6)	35 (1)
O(2)	5602 (4)	6568 (2)	4117 (4)	51 (1)
C(3)	8437 (6)	7213 (3)	7102 (6)	41 (1)
O(3)	8481 (5)	7210 (3)	8090 (5)	66 (1)

[a] Parameters marked with an asterisk denote atoms assigned anisotropic thermal parameters given as the isotropic equivalent displacement parameter defined as $U_{eq} = {}^1/_3\sum_i\sum_j U_{ij}a^*_i a^*_j a_i a_j$. [b] Occupancy (1)/(1a) = 0.6/0.4.

tation matrix were determined from a least-squares treatment of 20 accurately centered high-angle reflections ($26.0 < 2\theta < 30.0°$).[10] Intensity data of 9133 reflections were collected in the range $0 < \theta < 25°$, in ω–2θ mode, at variable scan speeds (1.37–2.75 deg min⁻¹) and scan width of 0.8 + 0.35 tan θ, with a maximum time per datum of 60 s. Standard reflections of 00$\bar{1}$, 020, and 200 were monitored every 180 min of X-ray exposure time and showed 2.3% random decay over the total period of 130.7 h. Corrections were made for Lorentz, monochromator and crystal polarization, background radiation effects but not for decay using the Structure Determination Package[11] running on a PDP 11/23+ computer. An empirical absorption correction was applied[12] using a 360° ψ-scan for nine reflections in the range $1.97 < \theta < 14.84°$. The cell parameter and systematic absences indicated[13a] that the space group was $P2_1/c$ and the correctness of the choice of the space group was confirmed by successful solution and refinement of the structure. The structure was solved with MULTAN[14] and subsequent difference Fourier techniques. Refinement on F was carried out by full-matrix least-squares techniques using the SHELX-76 software[15] running on a SUN 3/80 workstation. Scattering factors for neutral, non-hydrogen atoms were taken from ref 13b. Anisotropic thermal parameters were assigned for Rh, Co, and P atoms and were refined, while the thermal parameters of all the remaining non-hydrogen atoms were refined isotropically. The hydrogen atoms attached to the carbon atoms were introduced on calculated positions (C–H = 0.90 Å) and were included in the refinement riding on their carrier atoms. The hydride atom was located from a difference Fourier map unambiguously, and the positional and thermal parameters were refined in the least-squares cycles. The disorder in the BF_4^- anion was successfully resolved. With the use of 6160 observations with $I > 3\sigma(I)$ and the use of weights of the form $w = k/\sigma^2(F_o) + gF^2$ where $k = 2.2259$ and $g = 0.000\,606$, refinement of 219 variables converged at agreement factors $R = 0.0519$ and $R_w = 0.0558$. The top five peaks in the final difference Fourier synthesis with electron density in the range 0.805 to 0.712 e Å⁻³ and are associated with O(3), C(315), C(313), F(2), and C(215) at distances 0.57–0.78 Å. The experimental details and crystal data and selected positional and U(equiv) thermal parameters are given in Tables III and IV. Selected bond distances and angles are collected in Table I. More complete tables and tables of anisotropic thermal parameters, calculated hydrogen atom positional parameters, root-mean-square amplitudes of vibration, weighted least-squares planes and dihedral angles, selected torsion angles, and structure amplitudes have been deposited as supplementary material.

Acknowledgment. We thank the NSERC (Canada) for financial support and Dr. N. C. Payne for X-ray facilities.

Supplementary Material Available: A summary of the X-ray structure determination and tables of crystallographic data, atomic positional and thermal parameters, bond distances and angles, hydrogen atom positional parameters, least-squares planes, and torsion angles for **2** (9 pages); a table of observed and calculated structure factors for **2** (37 pages). Ordering information is given on any current masthead page.

(10) *CAD4 Diffractometer Manual*; Enraf-Nonius: Delft, The Netherlands, 1988.
(11) Enraf-Nonius Structure Determination Package, SDP-PLUS, Version 3.0. 1985.
(12) North, A. C. T.; Phillips, D. C.; Mathews, R. S. *Acta Crystallogr., Sect. A* **1968**, *24*, 351.
(13) *International Tables for X-ray Crystallography*: (a) Vol. A, D. Reidel Publishing Co.: Boston, MA, 1983; (b) Vol. IV, Kynoch Press: Birmingham, England, 1974.
(14) Main, P. MULTAN 82 Manual. 1982.
(15) Sheldrick, G. M. SHELX-76. Program for Crystal Structure Determination. University of Cambridge, England, 1976.

Contribution from the Department of Chemistry, University of Missouri—Kansas City, Kansas City, Missouri 64110

Electronic Structure Calculations on Octanuclear Silsesquioxanes and Aluminosilsesquioxanes

Clarke W. Earley

Received August 8, 1991

Semiempirical electronic structure calculations have been performed on a series of octanuclear molecular silicates and aluminosilicates to determine the effects of substitution of tetravalent silicon by trivalent aluminum. By inclusion of molecular species that have already been isolated and characterized, these calculated results have been compared directly with experimental values to determine the reliability of the results obtained. Although these calculations consistently predict Si–O bonds to be slightly longer than observed experimentally, they are shown to be quite successful at reproducing geometric trends within a related series of molecules. The calculated relative stabilities for compounds containing two or more aluminum atoms predict that isomers containing Al–O–Al linkages should be thermodynamically less stable, consistent with Loewenstein's rule for solid-state aluminosilicates. Selected studies of monoprotonated species have also been performed to determine the relative stability of different protonation sites, especially with regard to the proximity to aluminum. As expected, protonation of bridging oxygen atoms near trivalent aluminum sites is predicted to result in thermodynamically more stable, and thus less acidic, species than those produced by protonation of oxygen atoms bridging two tetravalent silicon atoms.

Introduction

Zeolites are aluminosilicates characterized by a framework structure containing open channels and cavities of molecular dimensions. They have found a number of industrial uses as adsorbents, ion-exchangers, and shape-selective catalysts. A variety of both naturally-occurring and synthetic zeolites are known, spanning a range of structural and physical properties. The physical properties of zeolites are known to be strongly dependent on the structure and composition of atoms present, and a large number of studies of zeolite structures and properties have

0020-1669/92/1331-1250$03.00/0